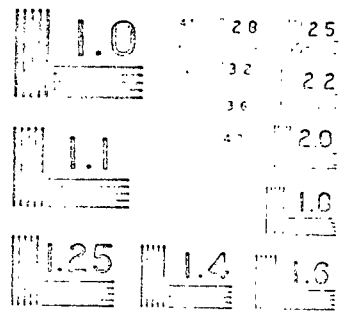

MICROCOPY RESOLUTION TEST CHART
NATIONAL BUREAU OF STANDARDS - 963

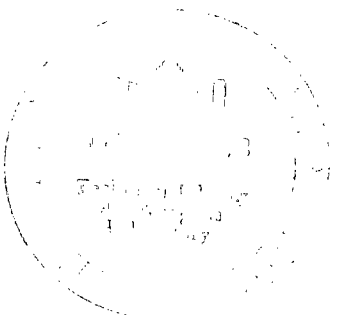

NASA TECHNICAL MEMORANDUM

NASA TM X- 68080

NASA TM X- 68080

(NASA-TM-X-68080) NASA-LEWIS EXPERIENCES WITH MULTIGROUP CROSS SECTIONS AND SHIELDING CALCULATIONS G.P. Lahti (NASA) 22 Jun. 1972 22 p CSCL 18F

N72-26531

Unclas
G3/22 33333

NASA-LEWIS EXPERIENCES WITH MULTIGROUP CROSS SECTIONS AND SHIELDING CALCULATIONS

by Gerald P. Lahti
Lewis Research Center
Cleveland, Ohio

TECHNICAL PAPER proposed for presentation at
American Nuclear Society Meeting
Las Vegas, Nevada, June 18-22, 1972

NASA-LEWIS EXPERIENCES WITH MULTIGROUP CROSS SECTIONS AND SHIELDING CALCULATIONS

Gerald P. Lahti
NASA-Lewis Research Center
Cleveland, Ohio 44135

SUMMARY

The nuclear reactor shield analysis procedures employed at NASA-Lewis are described. Emphasis is placed on the generation, use, and testing of multigroup cross section data. Although coupled neutron and gamma ray cross section sets are useful in two dimensional Sn transport calculations, much insight has been gained from examination of uncoupled calculations. These have led to experimental and analytic studies of areas deemed to be of first order importance to reactor shield calculations. A discussion is given of problems encountered in using multigroup cross sections in the resolved resonance energy range. The addition to ENDF files of calculated and/or measured neutron-energy-dependent capture gamma ray spectra for shielding calculations is questioned for the resonance region. Anomalies inherent in two dimensional Sn transport calculations which may overwhelm any cross section discrepancies are illustrated.

INTRODUCTION

NASA-Lewis has been involved in a number of nuclear reactor shield analyses. These include shields for a fast-spectrum space power reactor (ref. 1,2) and for a zirconium hydride reactor (ref. 3). The principal tools for these analyses are multigroup one- and two-dimensional discrete ordinates Sn transport codes. This paper will review our method of reactor shield analysis. Our technique of examining and testing of both basic data and cross section processing methods will be discussed. This paper will emphasize some problems we have encountered in generating and using broad multigroup cross sections in our day-to-day calculations. These problems are of importance to accurate reactor shield calculations and include the accuracy of MeV neutron transport and gamma ray production in the resolved resonance energy region. The purpose of this paper to alert and inform multigroup cross section measurers, code developers, and users regarding some of these subtle problems not covered adequately by existing codes.

USE OF COUPLED AND SEPARATE SHIELD DESIGN CALCULATIONS

The use of coupled neutron-and-gamma ray cross sections is a convenient method of simultaneously handling neutron transport and secondary gamma ray generation. Coupled cross sections save appreciable computer time and are used routinely in two dimensional transport calculations at NASA-Lewis. However, in the early design stages of any shield, one dimensional calculations are made without coupled cross sections to obtain input data necessary for efficient operation of our shield optimization procedures. Separate calculations are made for neutrons and gamma rays for each region and source type. This series of calculations displays the importance of each region to the total dose; thus the reactions and therefore the cross sections which are most important to a shield design may be ascertained. In a coupled calculation, this information is not available.

Here is a typical example of results from separate calulations (adapted from ref. 2) for the reactor shield configuration shown in figure 1. The spherical mockup of a 2 MWth fast spectrum space power reactor is reflected by 11 cm of molybdenum and shielded by four layers of lithium hydride and three layers of depleted uranium. The configuration has been optimized using the OPEX-II (ref. 4) procedure. The result is a minimum weight layered shield which meets a dose rate constraint of 2 millirem per hour 20 meters distant. The resulting configuration yields the dose rate distribution shown in figure 2. Each of the five radiation source regions contributes approximately equally to the total dose rate at the 20 meter detector position. Important contributions to the total dose rate are made from capture gammas formed deep in the shield. These are caused by MeV neutrons being transmitted to points deep in the shield, their local slowing down in the lithium hydride regions, and then their capture in the high-Z (uranium) layers. Examination of the balance tables in the Sn transport code output reveals that most of the neutron captures occur in the resonance energy region (i.e. 1 eV to 5 keV). Gamma rays from neutron inelastic scattering events represent a small fraction of the total dose rate. Thus in problems such as this, the transport of neutrons in the 6-15 MeV range to points deep in the shield, local slowing down, and resonance capture is the most important process as far as the dose rate at a distant external point is concerned. With this in mind, the cross sections, cross section codes, secondary gamma spectra, and transport methods which are available have been studied to evaluate their usefulness for precise shielding calculations.

EXAMINATION AND TESTING OF MeV-NEUTRON TRANSPORT METHODS

Data Base

There are several prerequisites to an accurate neutron transport calculation in the MeV energy region. First there is the precision of microscopic cross sections. Our basic source of neutron cross section data has been the B3 code, GAM-II, (ref. 5) and its 200 isotope library of data for the 0.4 eV to 15 MeV energy interval; for thermal neutron data, the P-1 code, GATHER-II (ref. 6) and its library of scattering kernels and other data has been utilized. The data here is of early 1960's vintage. GAM-II data files are presently being replaced using SUPERTOG-II (ref. 7) to generate updated decks from ENDF-Version II and III data. Secondly, the energy group split in the multigroup formulation is important because an infinite medium code (such as GAM-II) or a few-point one-dimensional cross section code (such as XSDRN (ref 8)) cannot adequately account for the spectrum shifts encountered in deep penetration problems. And finally, there is the uncertainty in the transport calculation itself due to the finite differencing.

Standard Group Splits and Cross Section Libraries

A standard 26 group split for neutrons (which includes 13 groups above 0.9 MeV and one thermal group, a 15 group split for gamma rays, and a 41 group coupled group split have been adopted for the shielding problems investigated here. Such a group split has proven to provide accuracy at least consistent with that of the Sn transport codes used. This also provides a reasonable balance between accuracy and running time required for transport problems. From previous work (ref. 9, for example), this particular group split tested well at deep penetrations in hydrogenous media against both finer calculations and experiments in the MeV region. These tests indicate the group split is adequate in this energy region for evaluating group fluxes and integral quantities such as dose for the types of problems at hand. Standard microscopic cross section libraries are maintained for easy access and quick running of our many survey calculations.

MeV Neutron Transmission Experiments

A number of thick sample transmission experiments have been performed at NASA-Lewis to test the adequacy of cross sections in the MeV energy region (ref. 9,10,11). These consist of either an americium-beryllium spherical neutron source surrounded by a spherical shell of material, or a 10 inch diameter cylindrical uranyl-fluoride, water solution reactor surrounded by a cylindrical shell or shells of material. Transmitted neutron spectra are measured using an NE-213 liquid scintillator system

and calculations are made with state-of-the-art one and two-dimensional Sn transport methods as they would be used in a shield design procedure. Reference 10 reports results for spherical shells of tantalum, tungsten, molybdenum, and beryllium. Major discrepancies between experiment and calculation were observed here, particularly for the case of beryllium (ENDF material 1007) and tantalum (ENDF material 1035). Figure 3 shows some representative results for the tungsten experiment. The discrepancies have been reported to the Cross Section Evaluation Working Group (CSEWG) for evaluation.

Reference 9 reports results of measurements and calculations for cylindrical shells of lead and water surrounding the reactor. The geometry and thicknesses in this experiment, shown in figure 4, are similar to space power reactor shields. The results calculated here, and shown in figure 5, used GAM cross sections. The agreement between experiment and calculation was reasonable; minor shape changes are observable upon close examination.

This type of cross section evaluation work is continuing here. Results of current experiments performed with spherical and cylindrical shells of lead and molybdenum are being reported at this meeting by Shook, et al (ref.11).

EXAMINATION OF METHODS OF INCLUDING SECONDARY GAMMA PRODUCTION

Data Base

Multigroup gamma ray transport cross sections are generated at Lewis using GAMLEG (ref. 12) along with LASL (ref. 13) or NBS (ref. 14) compilations of photo-electric and pair-production cross sections. Secondary gamma production cross sections are assembled from broad-group-averaged inelastic scattering and capture cross sections and an appropriate gamma spectra. Gamma spectra from thermal neutron capture and neutron inelastic scattering events used are basically from UNC compilations (ref 15), but are supplemented from various other current sources (ref 16). Coupled neutron-gamma ray cross section sets are assembled from this data using an undocumented set of computer codes.

Inelastic Scattering Gamma Ray Production Cross Sections

Inelastic scattering gamma ray production cross sections are assembled from:

1. GAM-II group averaged total inelastic scattering cross sections, and
2. the neutron-energy-dependent gamma ray spectra from inelastic scattering events tabulated in reference 15.

The latter data is utilized by reaveraging it to suit present neutron and gamma ray energy group splits. The averaging is performed using an undocumented code and assumes that the neutron flux per unit energy within any broad group is constant. Many of the gamma ray spectra here have been calculated and their precision is unknown. However, because of the small fraction of the total dose due to inelastic gamma rays in thick shields (see fig 2), such improvements would make only small changes in the total dose.

Capture Gamma Ray Production Cross Sections

There are several factors which affect the accuracy of capture gamma ray dose calculations. These include the accurate determination of the total number of captures, the spatial distribution of captures, especially in heavy shield layers, and the spectra emitted from these captures which is dependent on neutron energy. A great deal of attention (ref. 17) has been given recently to the measurement and calculation of capture gamma ray production cross sections. But little attention has been given to the calculation of the spatial distribution of captures especially in thick high-atomic-number resonance absorbers presently considered for high performance shields. The problems we have encountered in our studies of resonance capture of neutrons in layered shields (ref 18,19,20) is not of what spectra to employ, but of how to obtain appropriately averaged energy group capture cross sections for layers of resonance absorbers so as to insure that the correct total capture rate is conserved in each group.

The problem of precise calculation of the spatial distributions of neutron captures in resonance absorbers is of first-order importance because of the large gamma ray attenuation coefficient of these materials. Errors in spatial distribution of captures occur in multigroup transport calculations because of the necessarily broad energy groups employed. A single average capture cross section in each group, even if it correctly conserves total captures, must necessarily result in large underestimates of the capture rates at the surfaces of resonance absorbers. Consequently, the spatial distribution of capture events and gamma ray leakage will be in error.

It was pointed out in the discussion of figure 2 that for these optimized shields, a large portion of the total biological dose rate outside of the shield was due to resonance capture gamma rays born deep in the shield. Consider how a multigroup calculation handles resonance capture, for example, the 6.68 eV resonance in U-238. This might be contained in a broad group extending from 3 to 11 eV in a multigroup transport calculation. Figure 6 shows this cross section as calculated by the GAROL code (ref. 21) in a very fine group structure; this is representative of the continuous cross section in this energy interval. The requirement is to collapse this cross section to a single value for use in multigroup calculations through thick slabs of such resonance absorbing shield material. The cross section must be such that the total capture rate (neutron population) is conserved and the correct spatial distribution of captures (hence gamma leakage) is also conserved. To do both in a multigroup transport calculation with a reasonable number of energy groups is impossible. But one can at least conserve the total capture rate in the slab by employing a cross section calculated in a two-(or more) region resonance code such as GAROL and using multigroup cross section recipes consistent with the intended ultimate purpose of the cross section. Caution is advised for the shielder who uses multigroup cross sections because most of the cross section codes in existance have been written by reactor physics people. Formulations for multigroup cross sections in the resonance region as formulated in GAM-II, for example, give correct total capture rates only when absorber lumps, for which resonance calculations are made, are homogenized within a slowing down medium and subsequently are exposed to a 1/E flux in a transport or diffusion calculation. These cross sections were never intended to be used in a transport calculation through the lump. Users are advised to examine multigroup cross section recipes carefully before using them. Some details of our studies on this problem are included in reference 18.

One test of GAROL procedure has been made and reported in reference 18. The resulting capture distributions in a 3.14 cm depleted uranium slab surrounded by a pair of polyethylene slabs containing a 1/E neutron source is shown in figure 7. Shown is the capture rate in the 3-to-11 eV interval for the "exact" 10

group result along with that calculated with a one-group, GAROL-averaged cross section. The total capture rate has been conserved, but the spatial distribution of captures has not. In this case, the capture gamma leakage is underestimated by about 20 percent. (Total capture rates are incorrect if a broad group cross section is calculated in a one-region approximation and/or a formulation as coded in GAM-II is used in a transport calculation such as this.) GAROL-generated cross sections in the resonance region for use in our shielding calculations have been documented (ref. 19) and are available from RSIC as DLC-13 (GARLIB).

Bogart (ref. 20) has evolved an accurate method for calculating spatial capture distributions in thick layers of resonance absorbers surrounded by moderating media corresponding to layered shields. It employs multigroup effective resonance integrals calculated by GAROL to provide multigroup effective resonance cross sections. These cross sections are universal functions of distance into an absorbing layer. The method has worked remarkably well as shown in figure 8 where the measured spatial distribution of captures from cadmium cut-off to 100 keV for U-238 rods (ref 22) is compared to that calculated by Bogart. Such a technique has not yet been included in our routine coupled shielding transport calculations.

Neutron-Energy-Dependent Capture Gamma Ray Spectra

A definitive calculation has not yet been performed to conclusively demonstrate the importance of neutron energy dependent capture gamma ray spectra to a shielding calculation such as this. Furthermore, unless first-order changes are made in the method of calculating the spatial distribution of resonance captures in multigroup calculations, the inclusion of neutron-energy-dependent capture spectra in the resonance region is questionable.

Measured and calculated neutron energy dependent capture gamma ray spectra which are reported in broad neutron energy groups must be treated carefully. Such measurements have been made for the shield materials tungsten and uranium-238 (ref 23 and 24). For iron, a current re-evaluation (ref 25) for ENDF material 1124 includes calculated gamma ray energy distributions for 12 neutron energy groups. The measured data is generally reported as microscopic data but corresponds to averages over the finite sample measured, even though multiple neutron scattering corrections are made. The data is reported in broad neutron energy groups, each of which, in general, contains more than one resonance. Therefore, there is a question with regard to the applicability of this data to thick samples. In thick samples such as experienced in our layered shields, captures at the surface of a slabs are governed by the infinitely dilute resonance integral; nuclei within the slab see a depleted flux and captures are due to less peaked resonances, and the wings of

neighboring resonances. At every point within the slab, the neutron spectra is different than that impinging on the slab. Therefore, one can expect the capture gamma spectra to be different at any point within the slab. To do a proper averaging of both capture gamma spectrum and capture cross section for a given sized slab requires a cross section averaging code one step beyond any than is available (or even considered) today. Further, the problem of calculating the proper spatial distribution of captures (or an average cross section which permits the proper leakage of gammas) remains to be solved for use in routine multigroup calculations. Dudziak has recognized this in his infinitely-dilute gamma production cross section code, LAPHANO (ref. 26), and has allowed the user to input his own broad group weighting function to reflect all of the above mentioned phenomena.

NASA-Lewis Resonance Gamma Ray Production Cross Sections

Because of the complexities pointed out above, gamma production cross section cross sections in the resolved resonance energy region are generated at Lewis using broad group averaged neutron capture cross sections as calculated by GAROL, and the capture gamma ray spectra associated with the capture of thermal neutrons. This approach at least conserves the total number of resonance captures.

ANOMALIES IN 2-D TRANSPORT CALCULATIONS

Another problem in shield calculations is due to anomalies introduced in two dimensional transport calculations by ray effects and negative flux fix-ups. In reference 27, a series of two dimensional calculations was made for the reactor-shield configuration shown in figure 9. The geometry is only modestly irregular. Of interest was the biological dose rate at a distant point. To get this data, a two dimensional Sn transport calculation was performed to the outer boundary shown in the figure; then the leakage angular fluxes are integrated over the surface to obtain the dose rate at distant points. Figure 10 shows the neutron and gamma ray dose rates along the outer radial boundary of the transport problem as calculated for various angular quadrature orders. The undulations are due to ray effects generated in the void region. The location of the true dose rate distribution is unknown. Figure 11 shows the neutron and gamma ray dose rates along the bottom surface of the transport problem. The geometry is such that the dose rates should fall off monotonically with increasing radius. But a large spurious upturn is observable at the outer radius. This is due partially to ray effects, surface-to-surface streaming, and a net density reduction in the stepped region used to mock up the conical shield surface, but is mainly due to positive components of angular flux being generated in directions which, physically should have a zero value. These spurious sources appear in the void region due to negative flux fix-up procedures. In the void region, the magnitude of these angular fluxes is small compared to outward directed components. However by the time these spurious components are propagated to the bottom of the shield, they are larger than true angular fluxes which have been attenuated by the thick shield; hence, the spurious upturn. The uncertainties shown in figures 10 and 11 are much larger than any that would appear due to differences, say between ENDF and GAM cross section data. Again improvements in the routine transport procedures in use today must be made before improvements in cross section data can be seen in calculations such as this.

CROSS SECTION CODE PHILOSOPHY

Present efforts in cross section code development are toward major code systems which do all processing from point ENDF data to broad multigroup cross section files. However, with limited manpower at hand to write and/or maintain large cross section handling codes, the approach at Lewis has been to obtain well developed codes which require minimum debugging and maintainence. GAM-II, GATHER-II, GAMLEG, and SUPERTOG qualify here. We are also constrained by limited computing hardware, namely a pair of IBM 7094's and an IBM 360/67/TSS. Thus codes must be used which not only fit this hardware, but run in a reasonable length of time. Running a cross section code from the beginning (ENDF tape) to end (broad multigroup cross sections) in one pass is out of the question so the approach has been to run the separate modules individually. For example, run SUPERTOG to obtain GAM-II update decks (neutrons, 0.4 eV to 15 MeV), then update the GAM tape, then run GAM to obtain fast broad group cross sections, run GAMLEG to obtain gamma cross sections, et cetera, in separate runs, then combine all of the pieces to obtain the complete cross section deck. Although this process may take some time, many segments need be done only once. An example of the one-time-only run is the SUPERTOG to GAM run and the GAMLEG to multigroup gamma cross section run. Because each of these are for microscopic data for a given group split, they need be run only once for a given set of basic data for a given isotope. Mixing and merging of cross section sets can be done with simpler editing codes of local origin. This separate approach also permits more rapid substitution of individual cross section code modules in case the need to do so is deemed advisable. Thus, one is not "locked-in" to one major code system.

CONCLUDING REMARKS

In our studies of space power reactor shields, it has been useful to perform both coupled and separate calculations. Much insight has been obtained into the mechanisms of radiation transport and secondary gamma generation from separate calculations. These insights have led to experiments and analytic studies of areas most important to the design of space power reactor shields, namely neutron transport in the MeV region and resonance capture in thick resonance absorbers. Discrepancies between experiment and calculation in the MeV region have been found, in both GAM-II and ENDF data files.

The problem of how to handle resonance capture in a broad multigroup shielding calculation in a thick absorber has been studied and an approach has been taken which conserves the total capture rate within a region. But the spatial distribution of resonance captures within the absorber is grossly in error. This leads to erroneous gamma leakage from the absorber because of its very high gamma attenuation coefficient. The spatial capture problem not adequately handled in present codes. The incorporation in ENDF files of calculated or measured broad resolution gamma production cross sections for the resonance region is of questionable utility for the reactor shielding community.

It has been observed that large errors are introduced into a shielding calculation by

1. transport codes themselves as applied to even modestly irregular geometries due to ray effects and other anomalies, and
2. improper treatment of spatially dependent resonance absorption and erroneous generation of multigroup cross sections in the resonance region.

These effects may exceed errors due to uncertainties in the microscopic cross section data.

REFERENCES

1. Krasner, Morton H.; Davison, Harry W.; and Diaguila, Anthony J.: Conceptual Design of a Compact Fast Reactor for Space Power. Trans ANS, vol 14, no 1,1971,p.1.

2. Lahti, Gerald P.; and Herrmann, Paul F.: Comparison of Tungsten and Depleted Uranium in Minimum-Weight, Layered shields for a Space Power Reactor. NASA TM X-1874, Sept 1969.

3. Karp, I.M.; Soffer, L.; and Clark, M.R.: A Preliminary Shield Design for a SNAP-8 Power System. In "Proceedings of the National Symposium on Natural and Manmade Radiation in Space" NASA TM X-2440, Jan 1972, pp.78-83.

4. Lahti, Gerald P.: OPEX-II, A Radiation Shield Optimization Code. NASA TM X-1769, 1969.

5. Joanou, G.D.; and Dudek, J.S.: GAM-II, A B-3 Code for the Calculation of Fast-Neutron Spectra and Associated Multigroup Constants. GA-4265, Sept 1963.

6. Joanou, G.D.; Smith, C.V.; and Vieweg, H.A.: GATHER-II, An IBM-7090 FORTRAN-II Program for the Calculation of Thermal-Neutron Spectra and Associated Multigroup Cross sections. GA-4132, July 1963.

7. Wright, R.Q.; Lucius, J.L.; Greene, N.M.; and Craven Jr, C.W.: SUPERTOG, A Program to Generate Fine Group Constants and Pn Scattering Matrices from ENDF/B. ORNL-TM-2679, 1969.

8. Greene, N.M.; and Craven, Jr., C.W.: XSDRN: A Discrete Ordinates Spectral Averaging Code. ORNL-TM-2500. July 1969.

9. Lahti, Gerald P.; and Wrights, Gilbert N.: Measured and Calculated Fast-Neutron Spectra in a Lead-and-Water Shielded Reactor. NASA TM X-67861, June 1971. Also Trans ANS vol 14, no 1, June 1971, p.399.

10. Shook, D.F.; Fieno, D.; Ford, C.H.; and Alexander, R.L.: An Integral Test of Inelastic Scattering Cross Sections Using Measured Neutron Spectra from Thick Shells of Ta, W, Mo, and Be. In "Proceedings of the Third Conference on Neutron Cross Sections and Technology", CONF-710301 (Vol. I), pp. 98-105.

11. Shook, D.F.; Fieno, D.; and Ford, C.H.: An Integral Test of the Inelastic Cross Sections of Pb and Mo Using Measured Neutron Spectra. To be published. Also see Trans ANS vol 15, no 1, June 1972, pp. ???.

12. Lathrop, K.D.: GAMLEG- A FORTRAN Code to Produce Multigroup Cross Sections for Photon Transport Calculations. LA 3267, March 1965.

13. Storm, Ellery; and Israel, Harvey I.: Photon Cross Sections from 0.001 to 100 MeV for Elements 1 through 100. LA-3753, 1967.

14. Hubbell, J.H.: Photon Cross Sections, Attenuation Coefficients, and Energy Absorption Coefficients From 10 keV to 100 GeV. NSRDS-NBS 29, August 1969.

15. Celnik, J.; and Spielberg, D.: Gamma Spectral Data for Shielding and Heating Calculations. UNC-5140 (NASA CR-54794), Nov. 1965.

16. Ford, W.E. III: The POPOP4 Library of Neutron-Induced Secondary Gamma-Ray Yield and Cross Section Data. Union Carbide Report CTC-42, Sept. 1970.

17. Orphan, V.J.; John, Joseph; and Hoot, C.G.: Measurements of Gamma-Ray Production Cross Sections for Shielding Materials of Space Nuclear Systems. In "Proceedings of the National Symposium on Natural and Manmade Radiation in Space" NASA TM X-2440, Jan 1972, pp.500-511.

18. Lahti, Gerald P.: Multigroup Calculations of Resonance Neutron Capture in a Thick Slab of Depleted Uranium. NASA TM X-1878, Sept 1968. Also Trans ANS vol 12, no 1, June 1969, p.389.

19. Lahti, Gerald P.; and Westfall, Robert M.: Multigroup Resonance Region Cross Sections for Tungsten and Depleted Uranium for Use in Shielding Calculations. NASA TM X-1909, Jan 1970. Also Trans ANS vol 12, no 2, Dec 1969, p.964.

20. Bogart, Donald: Estimation of Spatial Distributions of Neutron Captures in Resonance Absorbers. NS&E vol 41, pp. 37-46(1970).

21. Stevens, C.A.; and Smith, C.V.: GAROL- A Computer Program for Evaluating Resonance Absorption Including Resonance Overlap. General Atomic Report GA-6637, Aug. 24, 1965.

22. Hellstrand, Eric: Measurement of the Effective Resonance Integral in Uranium Metal and Oxide in Different Geometries. J. Appl. Phys., vol.28, no.12, Dec. 1957, pp. 1493-1502.

23. Orphan, V.J.; and John,Joseph: Intensities of Gamma Rays from the Radiative Capture in Natural Tungsten of Neutrons from 0.02 eV to 100 keV. Gulf General Atomic Report GA-9121, Dec. 1968.

24. John, Joseph; and Orphan, V.J.: Gamma Rays from Resonant Capture of Neutrons in U-238. Gulf General Atomic Report GA-10186, June 1970.

25. Penny, S.K.; and Kinney, W.E.: A Re-evaluation of Natural Iron Neutron and Gamma-Ray Production Cross Sections--ENDF Material 1124. ORNL-4617 (ENDF-139), April 1971.

26. Dudziak, D.J.; Seamon, R.E.; and Susco, D.V.: LAPHANO: A Po Multigroup Photon-Production Matrix and Source Code for ENDF. LA-4750-MS (ENDF-156), Jan 1972.

27. Connolley, Donald J.; and Lahti, Gerald P.: Effect of Angular Quadrature on Results of Two-Dimensional Space Power Reactor Calculations. NASA TM X-67937, Oct 1971. Also Trans ANS , vol 14, no 2, Oct 1971, p.929.

REFERENCES

1. M. H. KRASNER, H. W. DAVISON, and A. J. DIAGULA, Trans. ANS, 14, 1 (1971).

2. G. P. LAHTI and P. F. HERRMANN, "Comparison of Tungsten and Depleted Uranium in Minimum-Weight, Layered shields for a Space Power Reactor", NASA TM X-1874 (1969).

3. I. M. KARP, L. SOFFER, and M. R. CLARK, in "Proceedings of the National Symposium on Natural and Manmade Radiation in Space", NASA TM X-2440 (1972), p. 78.

4. G. P. LAHTI, "OPEX-II, A Radiation Shield Optimization Code", NASA TM X-1769 (1969).

5. G. D. JOANOU and J. S. DUDEK, "GAM-II, A B-3 Code for the Calculation of Fast-Neutron Spectra and Associated Multigroup Constants", GA-4265, General Dynamics Corp. (1963).

6. G. D. JOANOU, C. V. SMITH, and H. A. VIEWEG, "GATHER-II, An IBM-7090 FORTRAN-II Program for the Calculation of Thermal-Neutron Spectra and Associated Multigroup Cross Sections", GA-4132, General Dynamics Corp. (1963).

7. R. Q. WRIGHT, J. L. LUCIUS, N. M. GREENE, and C. W. CRAVEN, Jr, "SUPERTOG, A Program to Generate Fine Group Constants and Pn Scattering Matrices from ENDF/B", ORNL-TM-2679, Oak Ridge National Lab. (1969).

8. N. M. GREENE and C. W. CRAVEN, Jr, "XSDRN: A Discrete Ordinates Spectral Averaging Code", ORNL-TM-2500, Oak Ridge National Lab. (1969).

9. G. P. LAHTI and G. N. WRIGHTS, "Measured and Calculated Fast-Neutron Spectra in a Lead-and-Water Shielded Reactor", NASA TM X-67861 (1971); Also Trans. ANS, 14, 399 (1971).

10. D. F. SHOOK, D. FIENO, C. H. FORD, and R. L. ALEXANDER, in "Proceedings of the Third Conference on Neutron Cross Sections and Technology", AEC CONF-710301, Vol. I (1971), p. 98.

11. D. F. SHOOK, D. FIENO, and C. H. FORD, "An Integral Test of the Inelastic Cross Sections of Pb and Mo Using Measured Neutron Spectra", To be published; Also Trans. ANS, 15 (June 1972).

12. K. D. LATHROP, "GAMLEG--A FORTRAN Code to Produce Multigroup Cross Sections for Photon Transport Calculations", LA-3267, Los Alamos Scientific Lab. (1965).

13. E. STORM and H. I. ISRAEL, "Photon Cross Sections from 0.001 to 100 MeV for Elements 1 through 100", LA-3753, Los Alamos Scientific Lab. (1967).

14. J. H. HUBBELL, "Photon Cross Sections, Attenuation Coefficients, and Energy Absorption Coefficients From 10 keV to 100 GeV", NSRDS-NBS 29, National Bureau of Standards (1969).

15. J. CELNIK and D. SPIELBERG, "Gamma Spectral Data for Shielding and Heating Calculations", UNC-5140, NASA CR-54794, United Nuclear Corp. (1965).

16. W. E. FORD, III, "The POPOP4 Library of Neutron-Induced Secondary Gamma-Ray Yield and Cross Section Data", CTC-42, Union Carbide Corp. (1970).

17. V. J. ORPHAN, J. JOHN, and C. G. HOOT, in "Proceedings of the National Symposium on Natural and Manmade Radiation in Space", NASA TM X-2440 (1972), p. 500.

18. G. P. LAHTI, "Multigroup Calculations of Resonance Neutron Capture in a Thick Slab of Depleted Uranium", NASA TM X-1878 (1968); Also Trans. ANS, 12, 389 (1969).

19. G. P. LAHTI and R. M. WESTFALL, "Multigroup Resonance Region Cross Sections for Tungsten and Depleted Uranium for Use in Shielding Calculations", NASA TM X-1909 (1970). Also Trans. ANS, 12, 964 (1969).

20. D.BOGART, Nucl. Sci. Eng., 41,37 (1970).

21. C. A. STEVENS and C. V. SMITH, "GAROL- A Computer Program for Evaluating Resonance Absorption Including Resonance Overlap", GA-6737, General Dynamics Corp. (1965).

22. E. HELLSTRAND, J. Appl. Phys., 28, 1493 (1957).

23. V. J. ORPHAN and J. JOHN, "Intensities of Gamma Rays from the Radiative Capture in Natural Tungsten of Neutrons from 0.02 eV to 100 keV", GA-9121, Gulf General Atomic, Inc. (1968).

24. J. JOHN and V. J. ORPHAN, "Gamma Rays from Resonant Capture of Neutrons in U-238", GA-10186, Gulf General Atomic, Inc. (1970).

25. S. K. PENNY and W. E. KINNEY, "A Re-evaluation of Natural Iron Neutron and Gamma-Ray Production Cross Sections--ENDF Material 1124", ORNL-4617, ENDF-139, Oak Ridge National Lab. (1971).

26. D. J. DUDZIAK, R. E. SEAMON, and D. V. SUSCO, "LAPHANO, A Po Multigroup Photon-Production Matrix and Source Code for ENDF", LA-4750-MS, ENDF-156, Los Alamos Scientific Lab. (1972).

27. D. J. CONNOLLEY and G. P. LAHTI, "Effect of Angular Quadrature on Results of Two-Dimensional Space Power Reactor Calculations", NASA TM X-67937 (1971); Also Trans. ANS, 14, 929 (1971).

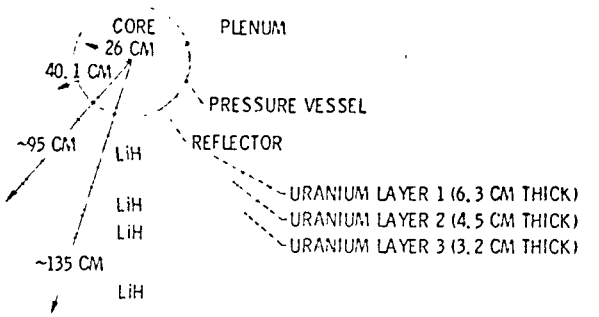

Figure 1. - Schematic representation of layered, spherical reactor and shield assembly. (Approx. to scale.)

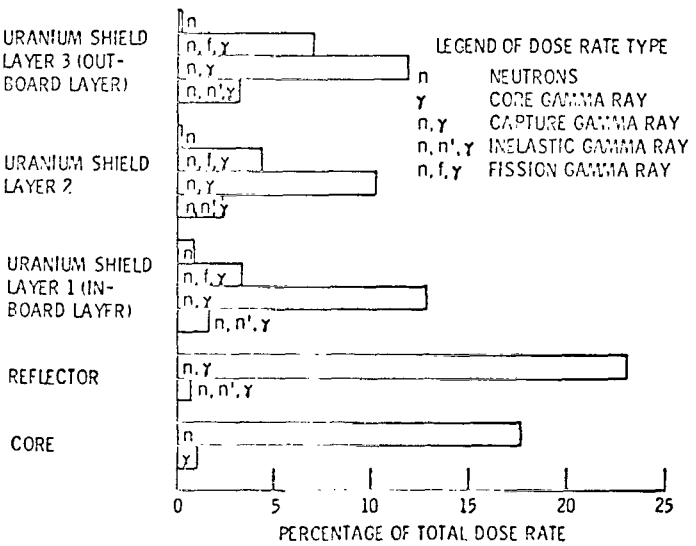

Figure 2. - Distribution of dose rate at detector by source region and source type for an optimized 7-layer LiH-depleted uranium shield (total dose rate 2 mrem/hr at 20 meters distant)(adapted from ref. 2).

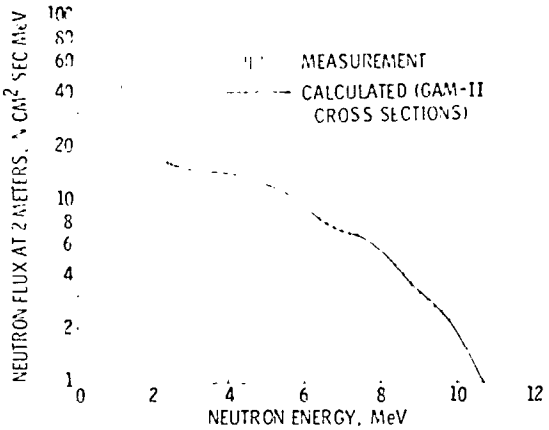

Figure 3. - Leakage spectrum for source enclosed by a 8.38 cm thick spherical shell of tungsten (density = 11.87 g/cm³) (from ref. 10).

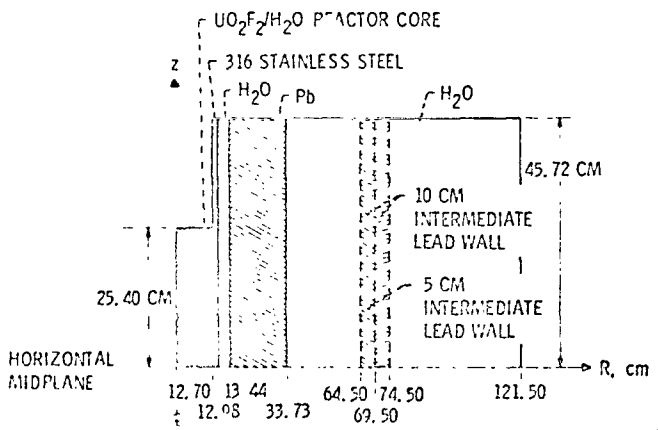

Figure 4. - Geometry of the NASA UO_2F_2/H_2O reactor surrounded by lead and water cylindrical shell shields. Region above horizontal midplane is shown. The geometry is symmetric about the midplane. (From ref. 9.)

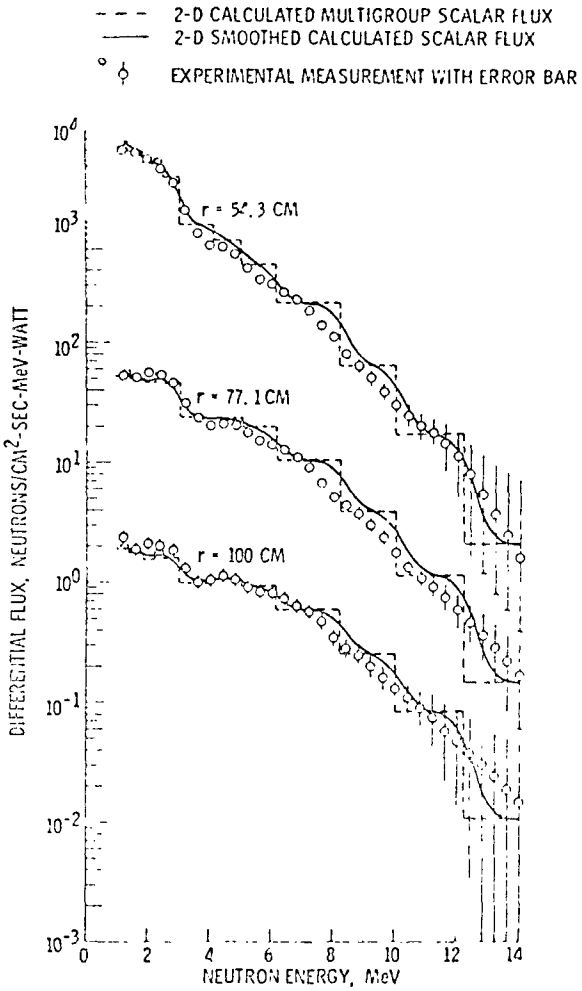

Figure 5. - Comparison of experimental and calculated results for reactor-20 cm lead-water configuration of figure 4. No intermediate lead in place. Calculations made in two dimensions with 13 energy groups, S_8 angular quadrature, and P_3 scattering. (From ref. 9.)

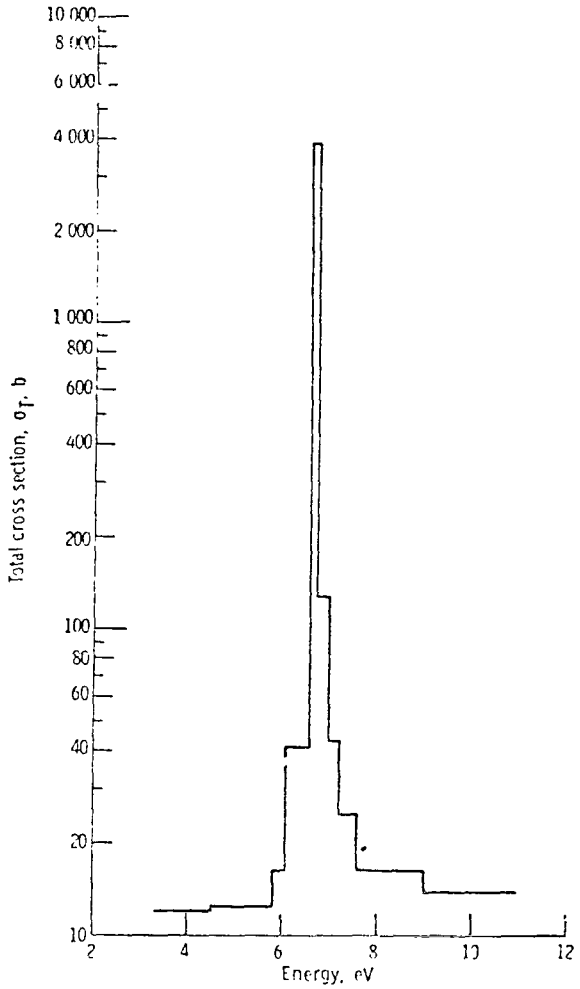

Figure 6. - Uranium-238 total cross section from 10-group-GAROL calculation. (From ref. 18.)

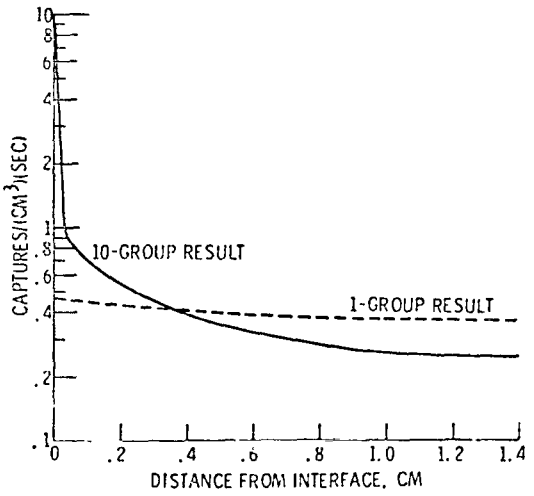

Figure 7. - Comparison of capture rate distribution in a 3.14 cm thick slab of U-238 calculated using 10 fine groups and one broad group over 3- to 11-eV neutron energy range. Both cross section sets calculated using the GAROL code. (From ref. 18.)

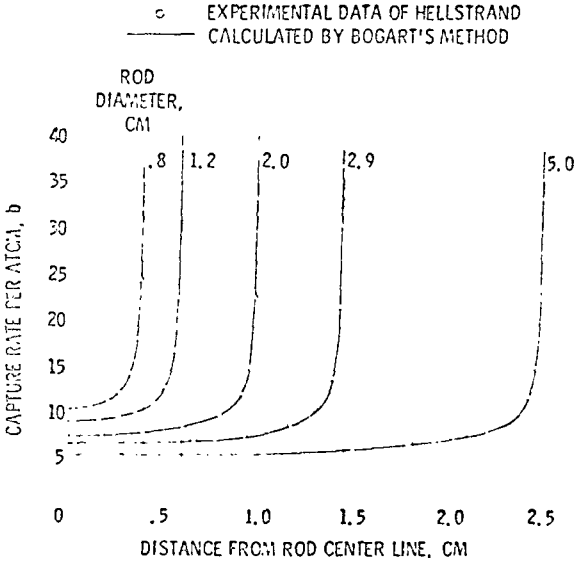

Figure 8. - Comparison of spatial distribution of captures calculated by Bogart's method with experimental data of Hellstrand for metallic rods of uranium-238. (From ref. 20.)

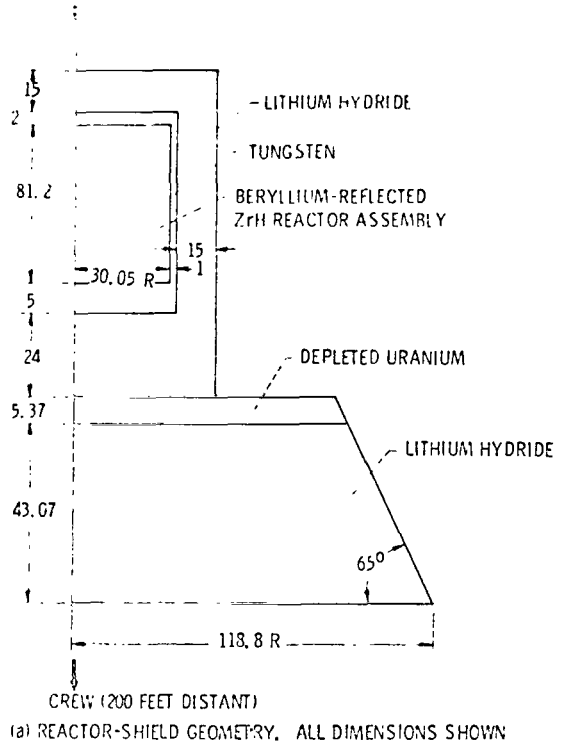

(a) REACTOR-SHIELD GEOMETRY. ALL DIMENSIONS SHOWN ARE IN CENTIMETERS.

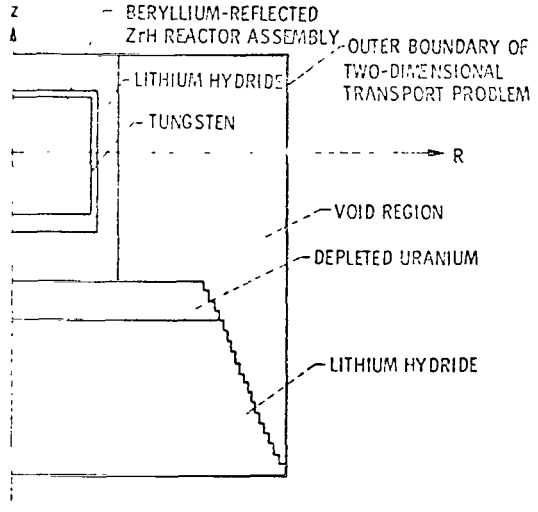

(b) R-Z MOCK-UP OF REACTOR-SHIELD GEOMETRY FOR 2-DIMENSIONAL TRANSPORT CALCULATIONS.

Figure 9. - Two dimensional space power reactor shield configuration and corresponding calculational model. (From ref. 27.)

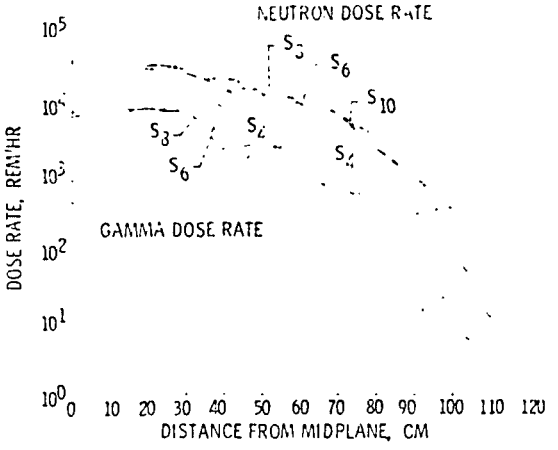

Figure 10. - Dose rates at radius 117 centimeter (near outer radial boundary of transport problem). Calculation are for P_2 scattering and various orders of angular quadrature denoted by n of Sn. (From ref. 27.)

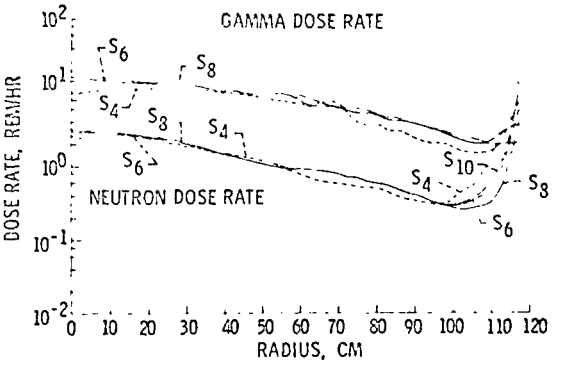

Figure 11. - Dose rates along bottom surface of shield. Calculations are for P_2 scattering and various orders of angular quadrature denoted by n of Sn. (From ref. 27.)

END

DATE

FILMED